Diabatic Heating's Influences on the Dynamics of Two Types of Extreme Precipitation in the Northeast United States

David Coe[1], Mathew Barlow[1], Laurie Agel[1]

[1]University of Massachusetts Lowell

1. Motivation and Method

Two extreme precipitation patterns for the Northeast U.S. (identified in Agel et al. 2019) were the result of a warm-conveyor belt and atmospheric river over the East Coast of the U.S. This study analyzes the influences that Diabatic Heating has on events in these two patterns, with a focus on Integrated Vapor Transport.

Here we provide an analysis of 20 storm events (10 in each pattern) run through a 48-hour WRF-ARW model with parameters as defined in section 2, identification of the two extreme precipitation patterns from Agel et al. (2019) section 3, an analysis of precipitation and synoptic composites between runs with and without Diabatic Heating in section 4, a comparison of Integrate Vapor Transport and the 250 hPa jet stream in section 5, and a preliminary look at the role Diabatic Heating plays in influencing 700 hPa vertical velocities in section 6.

The top 10 events that occurred after the year 2000 in each pattern were considered for this project (20 events total). GFS-FNL data was gathered for each date for 00z on the day prior to the event until 00z the day following the event. This data was then run in both a 27km and 9km WRF-ARW model with parameters defined in section 2.

2. WRF-ARW Model

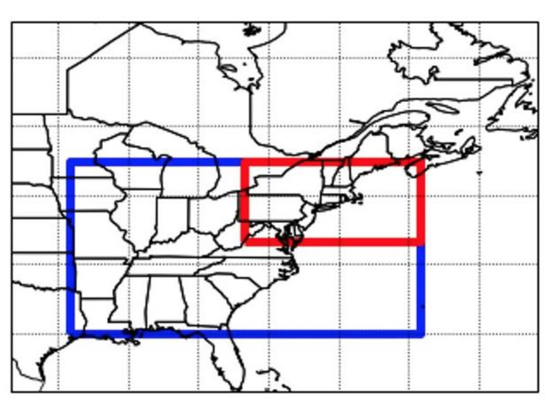

GFS-FNL data for the top 10 dates in each pattern after the year 2000 were gathered for this study from 00z the day prior to the event to 00z the day after the event. This data was then fed into the WRF-ARW model with the following parameters:

- 27km parent grid with 9 km child grid
- 2-way nesting
- mp_physics: (10) Morrison 2-moment scheme
- ra_lw_physics: (3) CAM scheme

The rest of the wrf namelist parameters were set to the pre-defined values in the provided namelist with the installation.

For runs without Diabatic Heating, these options were also used:

- cu_physics: no cumulus (0)
- Isfflx: no surface fluxes (0)
- no_mp_heating: microphysics heating options turned off (0)

3. Extreme Precipitation Patterns

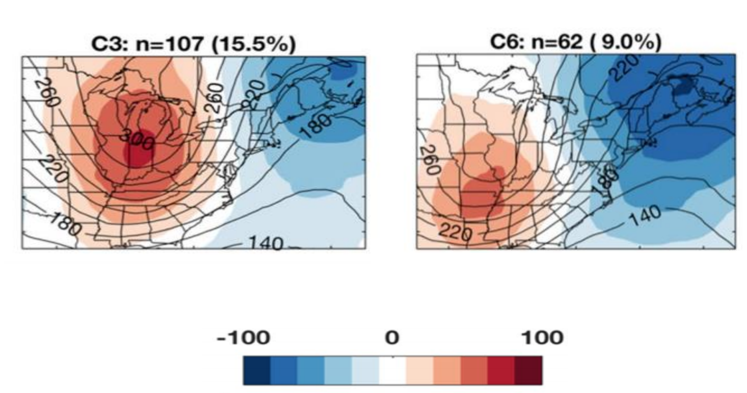

From Agel et al. (2019), 6 patterns were found using a k-means clustering technique on extreme precipitation events in the Northeast U.S. Of these patterns, C3 and C6 were selected for this study (figure above from Agel et al. 2019).

These two patterns were called "Ohio Valley troughs" and feature the deepest troughs of any of the extreme precipitation patterns. They both also feature the highest frequency of Warm Conveyor Belts in conjunction with extreme precipitation activity.

4. Precipitation and Synoptic Composites

Composites of daily precipitation (mm/dy) and average daily MSLP (hPa), daily precipitation, and average daily 500 hPa heights are shown in this section. Images feature the "Control" run with diabatic heating included on the left and runs with diabatic heating removed on the right.

The C3 diabatic heating removed composites features the axis of heaviest precipitation shifted west from the control run with a decrease in average daily precipitation. The 500 hPa heights saw relatively little difference, however the surface low is on average 4 mb weaker and less well defined in the diabatic heating removed composites.

The C6 diabatic heating removed composites feature the axis of precipitation shifted to the south and west of the control. In these runs, the surface low pressure has formed over the southern Ohio River Valley rather than over the East Coast, causing this shift.

C3 500 hPa height (red), MSLP (black), Precipitation (shaded)

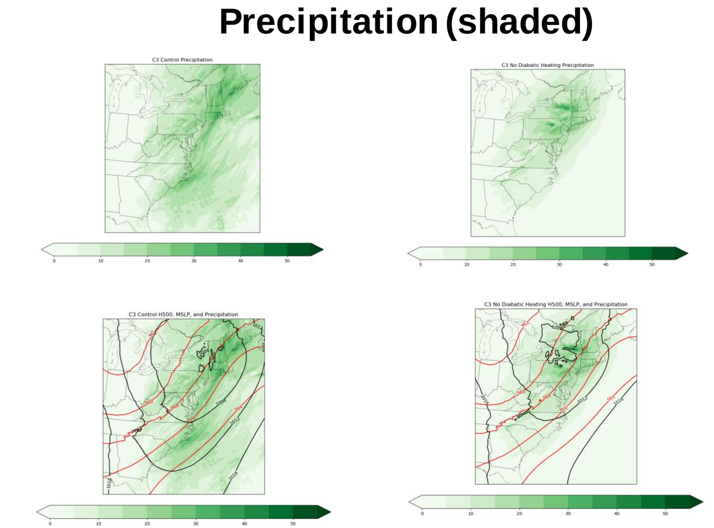

C6 500 hPa height (red), MSLP (black), Precipitation (shaded)

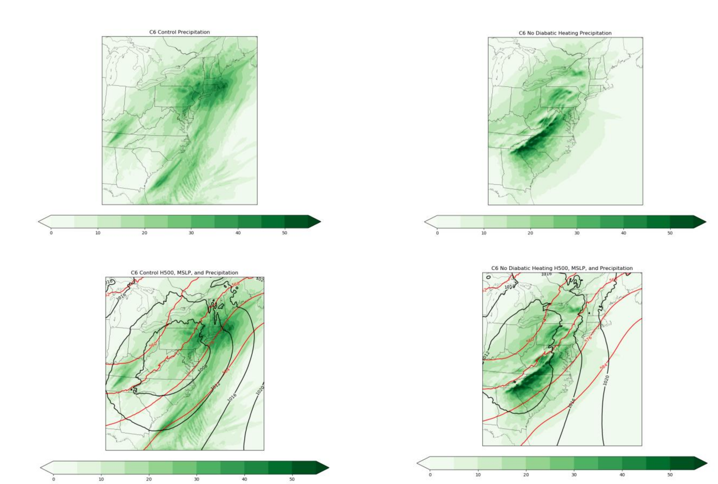

5. Integrated Vapor Transport (IVT) And 250 hPa Jet Stream

Composites of average daily IVT and average daily 250 hPa wind are shown in this section. Images feature the "Control" run with diabatic heating included on the left and runs featuring diabatic heating removed on the right.

The C3 diabatic heating removed composites feature weaker overall IVT with a much smaller total area of maximum IVT. The maximum IVT band is also shift further south and west. The 250 hPa jet is in a similar location, but on average 5-10 kts weaker with a smaller jet streak.

The C6 diabatic heating removed composites feature weaker overall IVT with the band of highest IVT values shifted to the west. The 250 hPa jet is in a similar location but note the lack of a jet streak in Northern New England in the diabatic heating removed composite.

C3 IVT (top, kg $m^{-1}s^{-1}$) and 250 hPa winds (bottom, kts)

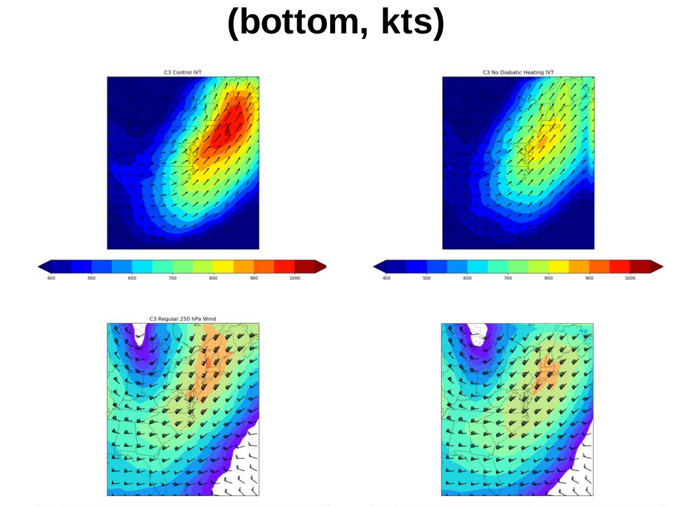

C6 IVT (top, kg $m^{-1}s^{-1}$) and 250 hPa winds (bottom, kts)

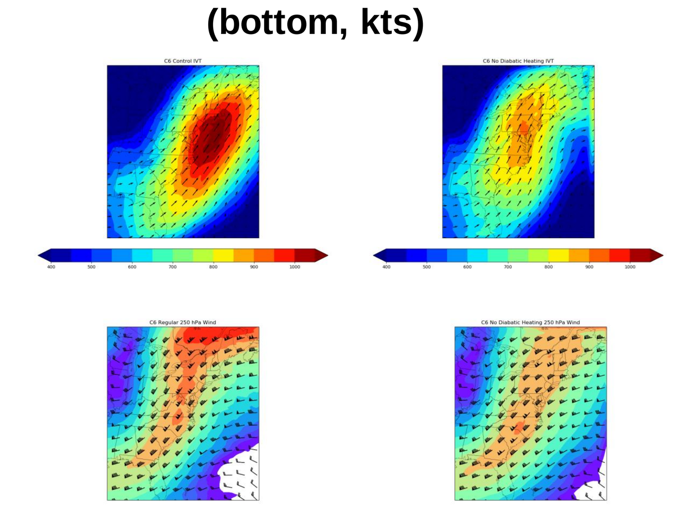

6. 700 hPa Vertical Velocity

A preliminary analysis of 700 hPa vertical velocity is shown in the panels to the right. Omega was extracted from the wrf files and converted to microbars per second and multiplied by (-1) to represent positive values as upward motion and negative values as downward motion.

Overall, removing diabatic heating resulted in stronger downward motion and weaker upward motion. Upward motion was also located further west in both cases compared to the control runs.

Due to time constraints, additional analysis is going to be performed related to Q-vectors for each case to understand the role diabatic heating plays in these systems.

C3 700 hPa Vertical Velocity (-1*μb s^{-1})

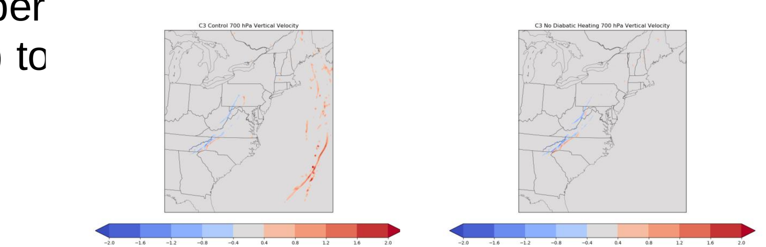

C6 700 hPa Vertical Velocity (-1*μb s^{-1}))

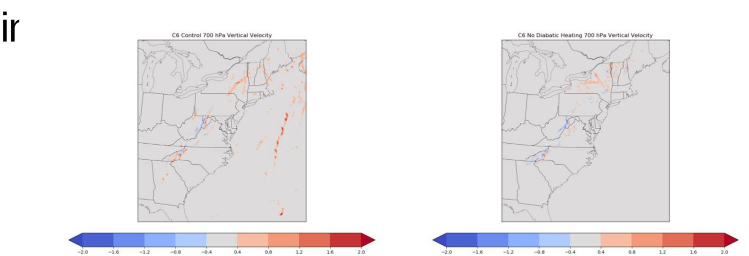

7. Discussion

Unsurprisingly, runs with diabatic heating removed featured a decrease in the overall precipitation and a weaker surface low pressure area.

The 500 hPa heights saw relatively no change in magnitude or location with diabatic heating removed. Even with no diabatic heating, the upper level trough was still located within the Ohio Valley Region with a similar magnitude.

Removing diabatic heating resulted in a weakening of the 250 hPa jet along with a reduction in IVT. Vertical velocity in the diabatic heating removed cases reflected the decrease in IVT, showing stronger downward motion, weaker upward motion, and a westward shift compared to the control cases.

8. References

Agel, L., Barlow, M., Colby, F. et al. 2019: Dynamical analysis of extreme precipitation in the US northeast based on large-scale meteorological patterns. *Clim. Dyn.*, in press

9. Acknowledgements

We gratefully acknowledge support by NSF AGS-1623912.

For more information, contact: David_Coe@student.uml.edu, @Daviology38, github.com/Daviology38